LA-UR 06-2765
astro-ph/0605271

Constraints on Sterile Neutrino Dark Matter

Kevork Abazajian
T-8 & T-6, Theoretical Division, MS B285, Los Alamos National Laboratory, Los Alamos, NM 87545, USA

Savvas M. Koushiappas
T-6, Theoretical Division, & ISR-1, ISR Division, MS B277, Los Alamos National Laboratory, Los Alamos, NM 87545, USA

We present a comprehensive analysis of constraints on the sterile neutrino as a dark matter candidate. The minimal production scenario with a standard thermal history and negligible cosmological lepton number is in conflict with conservative radiative decay constraints from the cosmic X-ray background in combination with stringent small-scale structure limits from the Lyman-alpha forest. We show that entropy release through massive particle decay after production does not alleviate these constraints. We further show that radiative decay constraints from local group dwarf galaxies are subject to large uncertainties in the dark matter density profile of these systems. Within the strongest set of constraints, resonant production of cold sterile neutrino dark matter in non-zero lepton number cosmologies remains allowed.

PACS numbers: 95.35.+d,14.60.Pq,14.60.St,98.65.-r

I. INTRODUCTION

The nature of the dark matter remains a fundamental problem in cosmology and particle physics. Much can be gained from the inferred non-gravitational properties of the dark matter such as its decay, annihilation, interaction cross-section with baryonic matter, and kinetic properties [1]. A class of candidate dark matter particles with no standard model interactions, but couplings to the standard model neutrinos via their mass generation mechanism, are the sterile neutrinos. Sterile neutrinos can be produced in the early universe via non-resonant matter-affected oscillations [2], or through a resonant mechanism if there exists a non-negligible lepton asymmetry [3].

Weak interaction singlets such as sterile neutrinos arise naturally in most extensions to the standard model of particle physics. Grand unified theories commonly contain singlets, which can act as sterile neutrinos, and can play a role in their mass-generation mechanism [4]. Several models contain light singlets as sterile neutrinos, including left-right symmetric (mirror) models [5], supersymmetric axinos as sterile neutrinos [6], superstring models [7], models with large extra dimensions [8, 9], and phenomenological models such as the νMSM [10]. Letting the mass and mixing angle between the sterile and respective active neutrino be free parameters, as well as the lepton number of the universe be free, the sterile neutrino can behave as hot, warm or cold dark matter, with masses in the range $\sim 0.1 - 100$ keV [11]. The abundance of sterile neutrinos and its relationship to the mixing parameters is affected by the quark-hadron transition, however, this relationship is well known for the standard prediction of a cross-over transition [12].

In the standard non-resonant production mechanism, sterile neutrinos are produced via a collision-dominated oscillation conversion of thermal active neutrinos. Deviations from a thermal spectrum in the sterile neutrinos are produced due to the change in the primordial plasma's time-temperature relation during production, dilution due to the disappearance of degrees of freedom, the modification of the neutrino thermal potential from the presence of thermal leptons, and the enhanced scattering rate on quarks above the quark-hadron transition [13]. As such, the resulting dark matter momentum distribution is suppressed and distorted from a thermal spectrum.

Sterile neutrinos exhibit a significant primordial velocity distribution. This has the effect of damping inhomogeneities on small scales and thus sterile neutrinos behave as warm dark matter (WDM). Models with a suppression of small scale power have drawn attention due to their potential alleviation of several unresolved problems in galaxy and small scale structure formation [14]. Of particular interest recently are the possible indications of the presence of cores in local group dwarf galaxies, inferred from the positions of central stellar globular clusters [15, 16] and radial stellar velocity dispersions [17]. The primordial velocity distribution produces a limit to the maximum phase-space packing of the dark matter, which, if attained, can produce a cored density profile for a dark matter halo. Conversely, this places a robust limit—the Tremaine-Gunn bound—on the mass and phase space of the dark matter particle from observed dynamics in galaxy centers [18].

Lighter mass WDM particles more easily escape gravitational potentials, and therefore suppress structure on larger scales, which can be constrained by the observed clustering on small scales of the Lyman-alpha (Lyα) forest. Possibly the most stringent limits on the suppression

of power on small scales are placed by inferring the small scale linear matter power spectrum from observations of the Lyα forest [19, 20, 21, 22]. The same flavor-mixing mechanism leading to the production of the sterile neutrino in the early universe leads to a radiative decay [23]. The decay rate increases as the fifth power of the mass eigenstate most closely associated with the sterile neutrino, and increases as the square of the mixing angle, producing a lighter mass neutrino and mono-energetic X-ray photon at half the dark matter particle mass. X-ray observations can either detect or constrain the presence of a line flux from surface mass densities of dark matter on the sky [24, 25]. So far, X-ray observations have placed upper limits on the particle mass and mixing angle relation of the dark matter sterile neutrino with observations of the cosmic X-ray background, clusters of galaxies, field galaxies, local dwarf galaxies and the Milky Way halo [26, 27, 28, 29, 30].

Sterile neutrinos lighter than those that may be the dark matter can also play a cosmological role as *hot* dark matter. One or more such light sterile neutrinos may be required to produce the flavor transformation seen in the Los Alamos Liquid Scintillator Neutrino Detector (LSND) experiment [31, 32]. Such sterile neutrinos would be associated with mass eigenstates of order 1 eV, and therefore much lighter than a warm or cold dark matter sterile neutrino. A light sterile neutrino of the type required by LSND would be thermalized in the early universe [33, 34], and is constrained by limits on the presence of hot dark matter from measures of large scale structure [35, 36]. Such limits can be avoided if the LSND-type sterile neutrino was not thermalized due to the existence of a small lepton number, though they nonetheless may be produced resonantly [37].

There are two other interesting physical effects when sterile neutrinos have parameters such that they are created as the dark matter in the non-resonant production mechanism. First, asymmetric sterile neutrino emission from a supernova core can assist in producing the observed large pulsar velocities above 1000 km s^{-1} [38, 39, 40]. The parameter space overlaps that of the non-resonant production mechanism (Fig. 1). Second, the slow radiative decay of the sterile neutrino dark matter in the standard production mechanism can augment the ionization fraction of the primordial gas at high-redshift (high-z) [41]. This can lead to an enhancement of molecular hydrogen formation and star formation, but also results in a strong increase in the temperature of the primordial gas [42]. This effect may have dire consequences on the formation of the first stars, which remains an open question [43].

In this paper, we review all of the constraints on the parameter space of the sterile neutrino as a dark matter candidate, in conjunction with the parameters needed for oscillation-based resonant and non-resonant production mechanisms for the sterile neutrino as the dark matter. In §II, we review the best current constraints on the sterile neutrino as a dark matter candidate. We review X-ray observation constraints in §II A. The most promising upper mass constraints come from X-ray observations of local group dwarfs, but we show that they are subject to significant uncertainties in the dark matter profile of the dwarf. In §II B, we discuss constraints from observations of the Lyα forest. This provides the most stringent lower mass constraints, which requires the free streaming length to be $\lesssim 90$ kpc$/h$, and forces the primordial velocity dispersion to be too small to sustain cored dark matter halos. With the combined constraints, we show that the standard zero-lepton number non-resonant production model is excluded if the most stringent constraints from the Lyα forest are combined with the most conservative decay limits of the X-ray background, and cannot be evaded in a model that dilutes and cools the dark matter sterile neutrino by massive particle decay [44]. However, we show that the combined constraints do not exclude resonant production mechanisms.

II. CONSTRAINTS

The non-resonant "zero" lepton-number production calculation presented in Ref. [13] is the simplest case model for the production of sterile neutrinos as dark matter candidates. In this model, there are no extra couplings postulated for the sterile neutrinos, and the cosmological lepton number is comparable to the baryon number, and thus negligible. The thermal history (up to temperatures of $T \sim 500$ MeV) is given by lattice QCD calculations through the quark-hadron transition, and contains no sterile neutrinos in the initial conditions of the plasma, due to the fact that the thermal potential suppresses sterile production at high temperatures.

In Fig. 1, we show contours of constant comoving density comparable to the dark matter density for the non-resonant zero lepton number ($L = 0$) case, as well as enhanced resonant production with initial cosmological lepton number cases ($L = 0.003$, $L = 0.01$, $L = 0.1$) from Ref. [12]. We have labeled the standard prediction of $L \sim 10^{-10}$ as nil since it is negligible for the non-resonant production mechanism. We define the lepton number as

$$L \equiv \frac{n_\nu - n_{\bar{\nu}}}{n_\gamma}, \tag{1}$$

where n_ν ($n_{\bar{\nu}}$) is the number density of the neutrino (antineutrino) flavor with which the sterile is mixed, and n_γ is the cosmological photon number density. The cosmological lepton number is limited by the inferred primordial helium abundance and the large to maximal mixing angle solutions to the solar and atmospheric neutrino problems: $|L_e| < 0.05$, $|L_\mu + L_\tau| < 0.4$ [46, 47, 48]. The constraints discussed below are framed around the parameter space required for the sterile neutrino dark matter production, and many are shown in Fig. 1.

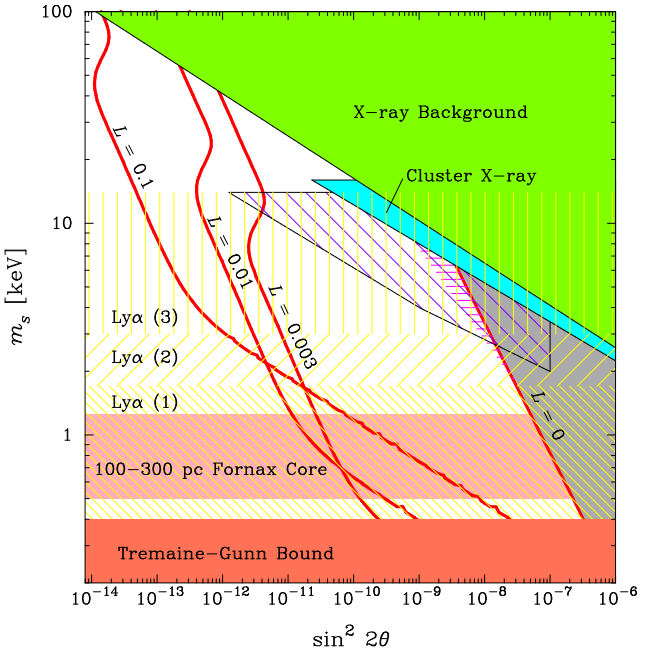

FIG. 1: Full parameter space constraints for the sterile neutrino production models, assuming sterile neutrinos constitute the dark matter. Contours labeled with lepton number $L = 0$, $L = 0.003$, $L = 0.01$, $L = 0.1$ are production predictions for constant comoving density of $\Omega_s = 0.24$ for $L = 0$, and $\Omega_s = 0.3$ for non-zero L [12]. Constraints from X-ray observations include the diffuse X-ray background (green) [27], from XMM-Newton observations of the Coma and Virgo clusters (light blue) [28]. The diagonal wide-hatched region is the claimed potential constraint from XMM-Newton observations of the LMC [29]. The region at $m_s < 0.4$ keV is ruled out by a conservative application of the Tremaine-Gunn bound [14]. The regions labeled Lyα are those from the amplitude and slope of matter power spectrum inferred from the SDSS Lyα forest [Lyα (1)] [21], using high-resolution Lyα data [Lyα (2)] [20, 21], and that from the high-z SDSS Lyα of SMMT [Lyα (3)] [22]. The grey region to the right of the $L = 0$ case is where sterile neutrino dark matter is overproduced. Also shown is the horizontal band of the mass scale consistent with producing a 100 - 300 pc core in the Fornax dwarf galaxy [45]. The parameters consistent with pulsar kick generation are in horizontal hatching [38, 39, 40].

A. X-ray measurements

In this section, we review the sterile neutrino dark matter constraints that come from measurements of the X-ray background, X-ray measurements from the Virgo and Coma clusters, as well as measurements of X-ray fluxes from the Draco local group dwarf.

It is straightforward to translate X-ray astronomy mass and mixing angle parameter space constraints to sterile neutrino mass constraints in the simplest model with the inversion of the production relation in Ref. [13]:

$$\sin^2 2\theta = 7.31 \times 10^{-8} \left(\frac{m_s}{\rm keV}\right)^{-1.63} \left(\frac{\Omega_s}{0.26}\right)^{0.813}, \quad (2)$$

where θ is the mixing angle between the active and sterile flavor states, and Ω_s is the fraction of the cosmological critical density in sterile neutrinos.

If sterile neutrinos constitute the density associated with dark matter, then their radiative decay would lead to a contribution to the X-ray background (XRB hereafter) [26]. In a recent analysis of the observed X-ray background from HEAO-1 and XMM-Newton, Boyarsky et al. [27] place the following limit on the particle mass and mixing angle,

$$\sin^2 2\theta < 1.15 \times 10^{-4} \left(\frac{m_s}{\rm keV}\right)^{-5} \left(\frac{\Omega_s}{0.26}\right), \quad (3)$$

with the corresponding exclusion region shown in Fig. 1. If we combine this result with the production Eq. (2), we find the corresponding upper mass limit to be

$$m_s < 8.9 \text{ keV}. \quad (4)$$

More stringent limits can be placed by X-ray observations of the large dark matter surface mass density in clusters of galaxies [26]. A recent analysis of XMM-Newton observations of the Virgo and Coma clusters was presented in Boyarsky et al. [28]. More specifically, it was shown that near the center of the Virgo cluster (at radial distances $r < 11$ arcmin), the X-ray flux places a rough power-law constraint on the $\sin^2 2\theta - m_s$ plane, as

$$\sin^2 2\theta < 10^{-2} \left(\frac{m_s}{\rm keV}\right)^{-6.64}. \quad (5)$$

If this result is combined with the production mass-mixing angle relation [Eq. (2)], it results in a particle mass constraint of [64]

$$m_s < 10.6 \text{ keV}. \quad (6)$$

The combined Virgo and Coma analysis of Boyarsky et al. [28] presents a more stringent limit. In this case, an approximate power-law fit to their exclusion region places a limit of

$$\sin^2 2\theta < 8 \times 10^{-5} \left(\frac{m_s}{\rm keV}\right)^{-5.43}, \quad (7)$$

which is considerably stronger than the XRB limit, Eq. (3). Using the production relation Eq. (2), this limit yields a sterile neutrino mass limit of

$$m_s < 6.3 \text{ keV}, \quad (8)$$

an improvement on the XRB limit, Eq. (4).

There are some notable issues with the Boyarsky et al. [28] analysis of the Virgo and Coma cluster data. The analysis uses a fixed phenomenological model for the X-ray emission of the cluster with specific lines added to fit atomic lines in the spectrum. On top of the phenomenological model, a Gaussian line representing the potential sterile neutrino flux is inserted with the width of the energy resolution of the instrument. This method does not

allow modeling of the energy-dependent resolution of the response of the detector, and can lead to a non-detection of a line feature that exists at the position of an atomic line. Emission lines could be more properly modeled for the gas in clusters by using a Mewe-Kaastra-Liedahl (MEKAL) model of the atomic and bremsstrahlung emission of the gas [49]. Nevertheless, barring the chance coincidence of the sterile neutrino emission feature lying on an instrumental feature or an atomic line, the limits, Eq. (7-8) from the Coma plus Virgo analysis of Ref. [28] should be robust.

We now discuss the prospects of detecting sterile neutrino dark matter in local dwarf galaxies. It was recently proposed by Boyarsky et al. [29] that X-ray observations by XMM-Newton of nearby local group dwarf galaxies may present the best opportunity for constraining or detecting the sterile neutrino decay flux of X-ray photons. The constraint region from that paper, using XMM-Newton observations of the Large Magellanic Cloud (LMC), is shown as the broad diagonal hatched region in Fig. 1.

Any analysis of the expected X-ray flux from sterile neutrino decays, such as in Ref. [29], is prone to the uncertainties in the dynamical estimate of the dark matter distribution in the dwarf galaxy [50]. For example, in the analysis of Ref. [51], the dark matter profile of the Draco dwarf galaxy is consistent with both cored and cusped dark matter distributions such as the NFW [52] and Burkert [53] profiles. These profiles may arise in the case of massive "cold" sterile neutrinos (NFW) or for lighter "warm" sterile neutrinos. In order to demonstrate the uncertainties in the X-ray flux due to the dark matter distribution in Draco, we show in Fig. 2 the value of the quantity $J[\Delta\Omega(\theta)]$ which is defined as the line of sight integral of the matter distribution over a solid angle $\Delta\Omega(\theta)$ centered on the dwarf galaxy and expressed as

$$J\left[\Delta\Omega(\theta)\right] = \rho_s \int_0^{2\pi} d\phi \int_0^{\theta} \sin\theta' \left[\int_{x_{\rm min}(\theta')}^{x_{\rm max}(\theta')} I[\tilde{r}(x)]\, dx\right] d\theta'. \quad (9)$$

Here, $I[\tilde{r}(x)]$ is a function which depends on the assumed dark matter profile, and takes the form of

$$I_{\rm NFW}\left[\tilde{r}(x)\right] = \frac{1}{\tilde{r}(x)\left[1+\tilde{r}(x)\right]^2} \quad (10)$$

$$I_{\rm BUR}\left[\tilde{r}(x)\right] = \frac{1}{\left[1+\tilde{r}(x)\right]\left[1+\tilde{r}^2(x)\right]}, \quad (11)$$

for the NFW and Burkert profiles respectively. In Eq. (9), ρ_s is the characteristic density of the assumed profile, the limits of the integration along the line of sight are $x_{\rm max,min}\theta = D\cos\theta \pm \sqrt{r_t^2 + (D\sin\theta)^2}$, the quantity $\tilde{r}$ is defined as $\tilde{r}(x) \equiv r(x)/r_s$, where r_s is the scale radius of the assumed profile, and it relates to the line of sight element through $\tilde{r}(x) = \sqrt{x^2 + D^2 - 2xD\cos\theta}$. The distance D to Draco is $D = [75.8 \pm 7 \pm 5.4]$ kpc estimated using RR Lyrae variable stars [54], and the tidal radius r_t is taken to be $r_t \approx 7\,$kpc. However, we point out that as long as $r_t \gg r_s$ the dependence of $\Delta\Omega(\theta)$ on r_t is weak.

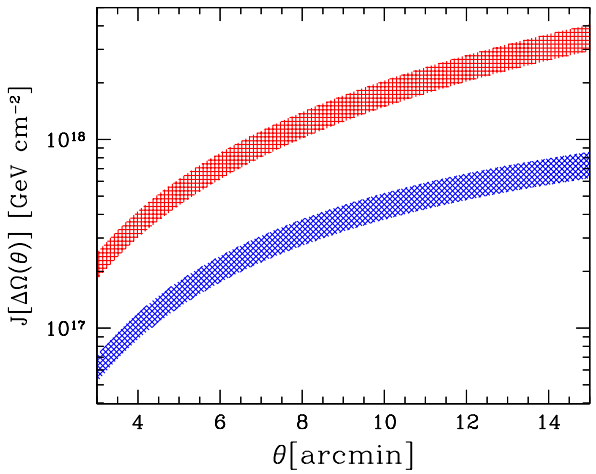

FIG. 2: The value of the quantity $J[\Delta\Omega(\theta)]$ (see text) for two representative dark matter distributions in the Draco dwarf galaxy. The thickness of both curves corresponds to the range of values in each profile due to the distance uncertainties to Draco. The top curve corresponds to an NFW profile with $\log(\rho_s/M_\odot{\rm kpc}^{-3}) = 7.0$ and $\log(r_s/{\rm kpc}) = 0.85$, while the lower curve depicts a Burkert profile with $\log(\rho_s/M_\odot{\rm kpc}^{-3}) = 9.0$ and $\log(r_s/{\rm kpc}) = -0.75$.

In Fig. 2 we show the value of the quantity $J[\Delta\Omega(\theta)]$ for two representative cases of a cored and cusped dark matter distributions. The top band depicts an NFW profile with $\log(\rho_s/M_\odot{\rm kpc}^{-3}) = 7.0$ and $\log(r_s/{\rm kpc}) = 0.85$, while the bottom band corresponds to a Burkert profile with $\log(\rho_s/M_\odot{\rm kpc}^{-3}) = 9.0$ and $\log(r_s/{\rm kpc}) = -0.75$. Both of these profiles are consistent with the observed line-of-sight velocity dispersion measurements as shown in [51]. Based only on profile and distance uncertainties, the value of the quantity $\Delta\Omega(\theta)$ varies between $[2.5 \times 10^{17} - 1.3 \times 10^{18}]{\rm GeV\,cm}^{-2}$, a factor of 5.2 at 8 arcmin (which corresponds roughly to the XMM field of view).

It has been claimed by Boyarsky et al. [29] that perhaps the X-ray flux from the LMC could provide the strongest constraint on the parameters of a sterile neutrino dark matter candidate. Modeling the distribution of dark matter in the inner regions of the LMC is even more uncertain due to the presence of a stellar disk and a bar (as for the Milky Way as well). As it was shown in numerous studies, e.g., Ref. [55], the LMC is baryon dominated in the central region, with a mass-to-light ratio of ~ 3 within the inner ~ 9 kpc (for comparison, dwarf spheroidals have mass-to-light ratios of ~ 100). The importance of baryon domination on the distribution of dark matter in the LMC was shown in the analysis of Ref. [56]. The derived mass of the LMC is uncertain to within 20%, depending on whether the disk is modeled as "maximal," or "minimal." If the baryons are dominating, then the rotation curve is much less sensitive to the

distribution of dark matter, making any estimate of the dark matter mass of the the LMC unreliable. In light of these uncertainties, we conclude that the LMC is an unreliable Milky Way satellite for robust X-ray constraints from detection of sterile neutrino decays.

Blank sky observations by X-ray telescopes may also provide a detectable dark matter decay flux due to the dark matter halo of the Milky Way itself [29, 30]. The importance of uncertainties in the dark matter profile of the Milky Way halo can also be significant. Models of the measures of the dynamics of the Milky Way can fit a range of halo masses of $(0.7-2)\times 10^{12} M_{\odot}$ [57, 58]. The uncertainty in these dynamical estimates can lead to a factor of 3 difference in the expected X-ray flux in directions perpendicular to the galactic plane, though these uncertainties are not reflected in the analyses of Refs. [29, 30].

B. Lyman-alpha Forest

The standard paradigm of cosmological structure formation is the gravitational growth and eventual collapse from small to large scales of initially adiabatic, Gaussian density fluctuations. WDM particle candidates alter the initial conditions of the perturbation spectrum by damping small scale fluctuations below the free streaming scale of the WDM. The sterile neutrino particle mass is constrained from below by the observations of small scale cosmological structure.

The most stringent lower bounds on the sterile neutrino mass arise from observations of the clustering of gas along the line of sight to distant quasars. The density fluctuations of the gas follow that of the dark matter to the scale at which the gas becomes pressure supported. The density fluctuations are linear to mildly nonlinear, and can probe extremely small scale dark matter fluctuations.

Using a combination of cosmic microwave background observations, the shape of the 3D power spectrum of galaxies from the Sloan Digital Sky Survey (SDSS), the inferred linear matter power spectrum amplitude and slope from the SDSS Lyα forest, the lower limit on the sterile neutrino particle mass is $m_s > 1.7$ keV (95% CL). In this limit, a linear bias relation between the Lyα flux power spectrum and matter power spectrum was assumed [21]. Using the inferred matter power spectrum from high-resolution spectra of the Lyα forest, the limit was improved to $m_s > 3.0$ keV (95% CL); however, significant systematic uncertainties exist in modeling the high-resolution data [21]. Seljak et al. [22] (hereafter SMMT) find a much more stringent constraint when directly using high-z flux power spectra from the SDSS measured by McDonald et al. [59] and other higher-resolution flux power spectra:

$$m_s > 14 \text{ keV (95\% CL)}. \tag{12}$$

All of these Lyα constraints are shown in Fig. 1.

Pioneering work on the sterile neutrino dark matter transfer function, using the approximation of a suppressed thermal sterile neutrino distribution, was done by Refs. [60, 61]. It has been shown that the sterile neutrino momentum distribution is not simply a suppressed thermal distribution, but is significantly nonthermal due to the effects on production of the dark matter by the changing particle population in the early universe, lepton population affecting the neutrino thermal potential, the quark-hadron transition, and the dilution of the dark matter due to particle annihilation [13, 26]. All of the above Lyα constraints use either the appropriate nonthermal transfer function for sterile neutrinos modified by their production at high temperatures in the early universe at or near the quark-hadron transition [13]. SMMT include an approximation to these effects via an augmentation in the sterile neutrino particle mass of 10%, since the above effects cool the momentum distribution. The original assumption of a simple suppressed thermal distribution for the sterile neutrino produces a suppression scale that is altered by a factor of order 10% in the particle mass of the sterile neutrino, though the correction increases with sterile neutrino particle mass due to their production at higher temperatures where all of the above effects are more pronounced. All of the physical effects producing a nonthermal distribution where included in the transfer function fit given in Ref. [13].

The strength of the SMMT results arises from the sensitivity of the high-z Lyα flux power spectra to changes in the 1D linear matter power spectrum, which is itself more sensitive to the suppression scale of WDM than the 3D power spectrum. At high-z, the recovery of the amplitude of the power spectrum via nonlinear clustering is reduced, enhancing the effects of WDM suppression. The temperature-density relation of the gas is constrained simultaneously by the observations in SMMT, though the strong change in the thermal state of the gas due to radiative sterile neutrino decay may be significant [42]. Another essential feature of the analysis in SMMT is the use of smaller volume hydrodynamical simulations that can resolve the very small free-streaming scale of 14 keV neutrinos. The free streaming scale of a sterile neutrino WDM is [11]

$$\lambda_{\rm FS} \approx 840 \text{ kpc}/h \left(\frac{\text{keV}}{m_s}\right)\left(\frac{\langle p/T\rangle}{3.15}\right), \tag{13}$$

where m_s is the mass state closely associated with the sterile neutrino flavor, and $\langle p/T\rangle$ is the mean momentum over temperature of the sterile neutrino distribution, and h is the Hubble parameter in units of 100 km s^{-1} Mpc^{-1}. A thermal WDM particle is defined such that $\langle p/T\rangle/3.15 \approx 1$. Due to the thermal history of the universe during production, the standard non-resonant production mechanism produces a "cool" sterile neutrino distribution, $\langle p/T\rangle/3.15 \approx 0.9$ [13], while the resonant production mechanism enhances low-p production, and $\langle p/T\rangle/3.15 \approx 0.6$, depending sensitively on the mass of the neutrino and initial lepton number [11].

The mass scale within the free streaming length is

$$M_{\rm FS} \approx 2.6 \times 10^{10}\ M_\odot/h\ \left(\frac{\Omega_m h^2}{0.14}\right)\left(\frac{\rm keV}{m_\nu}\right)^3\left(\frac{\langle p/T\rangle}{3.15}\right)^3, \quad (14)$$

where Ω_m is the fraction of the cosmological critical density in matter.

To resolve the required $\lambda_{\rm FS} \approx 54$ kpc$/h$ of a 14 keV neutrino, SMMT use a 20 Mpc h^{-1} box with 256^3 particles in dark matter and 512^3 cells for gas, providing a grid spacing of 39 kpc h^{-1}. This allows only for a resolution of a fraction of the suppression due to free streaming. Higher resolution in principle should only enhance the effects of the WDM suppression. To test convergence, SMMT use a single smaller volume simulation (10 Mpc h^{-1}) with the same particle and grid spacing and find a ∼20% change in the magnitude of the effect, though no higher resolution simulations were performed to test if the change is subsequently smaller as would be expected in numerical convergence. In addition, two other physical effects are degenerate, to different extents, with the effects of WDM, namely, pressure support due to the Jeans scale of the gas, and temperature broadening. These can mimic or hide the effects of the free streaming scale of the WDM, therefore the thermal properties of the gas are crucial to properly model in such limits.

A recent analysis by Viel et al. [62] (herafter VLHMR) used the same data of the SDSS Lyα flux power spectrum of McDonald et al. [59], but excluding higher resolution data used by SMMT. VLHMR utilizes a different method of mapping the response of the flux power spectrum to changes in cosmological and astrophysical parameters, *viz.*, VLHMR uses a parameterized Taylor series expansion of the flux power response to changes in physical paramters, with the Taylor parameters fit by numerical simulations. This method was shown to give similar results for the standard ΛCDM cosmology [63]. VLHMR finds a weaker sterile neutino particle mass lower limit, 10 keV (95% CL), than that of SMMT, 12 keV (95% CL), using the Lyα data from SDSS alone. The discrepancy with SMMT is increased when taking into account that the limit from VLHMR is too strong by $\gtrsim$10% because they do not use the correction for the "cooler" nonthermal spectrum of the sterile neutrinos due to the effects in the early universe described above. Overall, between the two analyses there exists a discrepancy of $\gtrsim$ 30% in the limits on the sterile neutrino mass. This could arise due to different CMB and galaxy data sets used: SMMT employs WMAP first year data and the SDSS galaxy power spectrum; VLHMR employs WMAP third year data, higher resolution CMB measurements and the 2dF galaxy power spectrum. Therefore, it is not certain whether the different CMB and galaxy data sets are the source of the discrepancy, or whether it is in the hydrodynamical simulations and method of mapping the response of the flux power spectrum to changes in physical parameters. However, both analyses find a stringent limit due to the precision of the measurement of the McDonald et al. [59] flux power spectrum at high redshift.

To reflect back on one of the principle motivations for WDM, it is important to note that it was shown by Strigari et al. [45] that if the constraints from Ref. [21], and especially SMMT are valid, then dynamical constraints from the Fornax dwarf galaxies limit the size of a core to be $\lesssim$ 85 pc and $\ll$ 10 pc for the two Lyα limits, respectively. In Fig. 1 we show the particle mass required to produce a [100-300] pc core by inverting the dynamical constraints of Strigari et al. [45]. These constraints by Strigari et al. are based on the inferred dark matter density profile from the radial velocity dispersion profile. The positions of the globular clusters in Fornax may indicate a core of ∼240 pc [15, 16]. Furthermore, the SMMT particle mass limit also limits the scale of the suppression of the halo mass scale to be well below the typical masses of dwarf galaxies, $M_{\rm FS} < 10^7 M_\odot\ {\rm h}^{-1}$.

In the resonant production model, the exact level of the lower bound from the Lyα forest would be modified for each lepton number case due to variation of $\langle p/T\rangle/3.15$ and therefore $\lambda_{\rm FS}$ for each case. However, this is at the level of ∼30% and is not monotonic across the lepton number region in $m_s - \sin^2 2\theta$ space. Therefore, we leave Lyα forest as a horizontal line in Fig. 1, to provide a rough guide to the limit. As shown in Fig. 1, even with the inclusion of all constraints, the resonant production model remains unconstrained at high-mass scales: $14 \lesssim m_s \lesssim 100$ keV.

To summarize, the results of SMMT are extremely significant, ruling out much of the parameter space that motivates WDM in general, and when combined with conservative X-ray bounds, as shown above, they rule out the standard sterile neutrino production mechanism. Therefore, there is strong motivation to verify the robustness of the SDSS Lyα measurements employed by SMMT as well as the modeling by hydrodynamic simulations.

III. CONSTRAINTS IN A DILUTION SCENARIO

It has been proposed that the production of sterile neutrino dark matter could be followed by the decay of a massive particle, whose decay products reheat the coupled species in the plasma, dilute the sterile neutrino dark matter and cool it relative to the coupled species [44]. Though this involves a conspiracy between the lifetime of the massive species and parameters coupling the sterile neutrino to the active sector, it is an interesting possibility that may alleviate structure formation constraints on the sterile neutrino. However, it is important to note that it does not allow a window for *warm* dark matter, as this mechanism *cools* the WDM particle until it may be consistent with structure formation limits.

In this scenario, a massive particle ($m \sim 100$ GeV) decays so that the entropy release changes the relative abundance of the dark matter by a factor S, i.e. $\Omega_s \rightarrow \Omega_s/S$. In the non-resonant oscillation production model,

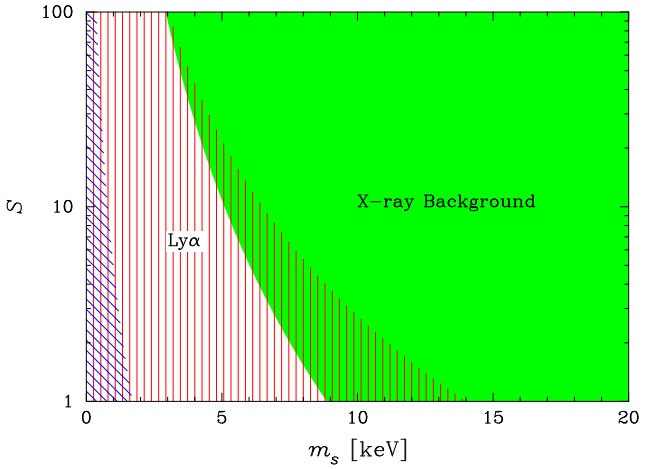

FIG. 3: Shown here are the constraints on the massive particle decay dilution model. The diagonally-hatched (blue) region is the lower-mass Lyα limit of Ref. [21], while the vertically (red) hatched region the Lyα limit of SMMT. In combination with the conservative XRB limit (green) [27], even extreme dilution models of $S = 100$ are in conflict with combined constraints. The standard case of no dilution corresponds to $S = 1$.

requiring a subsequent increase in the mixing angle of the production relation to

$$\sin^2 2\theta = 7.31 \times 10^{-8}\ S^{0.813} \left(\frac{m_s}{\rm keV}\right)^{-1.63} \left(\frac{\Omega_s}{0.26}\right)^{0.813}, \tag{15}$$

from Eq. (2). Using this and the conservative XRB limit, Eq. (3), the limit on the entropy release factor is

$$S < 8.6 \times 10^3 \left(\frac{m_s}{\rm keV}\right)^{-4.15} \left(\frac{\Omega_s}{0.26}\right)^{-2.23}, \tag{16}$$

which is valid for the mass range $1 \leq m_s \leq 100$ keV. With extended models, S can be as large as 100, at which point the dilution is occurring for sterile neutrinos that were at or nearly at thermal equilibrium with the plasma prior to the massive particle decay. Using Eq. (16) and the case where $S = 100$, the limit on sterile neutrino dark matter from the XRB is

$$m_s^{\rm entropy} < 2.9 \text{ keV}. \tag{17}$$

Limits from cosmological structure such as the Lyα forest are also modified by the cooling of the sterile neutrino free streaming length due to entropy release, such that the new lower mass limit is

$$m_s^{\rm entropy} = m_s^{\rm standard}\ S^{-1/3}. \tag{18}$$

For the most stringent Lyα forest limit of SMMT, Eq. (12), the entropy release model lower limit at $S = 100$ is

$$m_s^{\rm entropy} > 3.0 \text{ keV}. \tag{19}$$

This is in conflict with the XRB in the entropy release model, Eq. (17). The scaling of these relations is illustrated in Fig. 3. More stringent limits from X-ray clusters or local group galaxies would be in stronger conflict with Eq. (19). Blank-sky observations including contributions from the Milky Way halo also constrain high S models [30]. As such, we conclude that massive particle decay does not open a new window for the non-resonant oscillation production scenario.

IV. CONCLUSIONS

We have provided a comprehensive analysis of constraints on the parameter space of interest for the non-resonant and resonant production mechanisms of sterile neutrino dark matter. Observations in the X-ray of clusters of galaxies and the XRB place a limit to the radiative decay rate of a sterile neutrino candidate and provide constraints in the upper mass scale of the sterile neutrino dark matter. We have shown that limits from local group dwarf galaxies are subject to large uncertainties in the dark matter profile of these objects. The lack of the effects of the suppression of small scale power in the Lyα forest stringently limits the low mass scale region of parameter space.

The SDSS Lyα constraints from the analysis of SMMT, when combined with X-ray constraints, are in conflict with the sterile neutrino being the dark matter in the standard non-resonant zero lepton number production model. The SMMT limits also exclude much of the parameter space of interest for general WDM models. Non-zero lepton number cosmologies remain allowed for resonant production of "cold" sterile neutrino dark matter. We find, however, that dilution scenarios do not open a window for sterile neutrino dark matter. If the X-ray and Lyα constraints remain robust, then only non-zero lepton number cosmologies remain viable for the oscillation-production models of sterile neutrino dark matter.

Acknowledgments

We would like to to thank Peter Biermann, Alexey Boyarsky, James Bullock, George Fuller, Katrin Heitmann, Lam Hui, Alex Kusenko, Julien Lesgourgues, Maxim Markevitch, Uroš Seljak, Louie Strigari and John Tomsick for useful discussions. KA would like to thank the organizers of the Sterile Neutrinos in Astrophysics and Cosmology 2006 Workshop, where many of these discussions took place. This work was supported by Los Alamos National Laboratory under DOE contract W-7405-ENG-36.

[1] G. Bertone, D. Hooper, and J. Silk, Phys. Rept. **405**, 279 (2005), hep-ph/0404175.
[2] S. Dodelson and L. M. Widrow, Phys. Rev. Lett. **72**, 17 (1994), hep-ph/9303287.
[3] X.-d. Shi and G. M. Fuller, Phys. Rev. Lett. **82**, 2832 (1999), astro-ph/9810076.
[4] B. Brahmachari and R. N. Mohapatra, Phys. Lett. **B437**, 100 (1998), hep-ph/9805429.
[5] Z. G. Berezhiani and R. N. Mohapatra, Phys. Rev. **D52**, 6607 (1995), hep-ph/9505385.
[6] E. J. Chun and H. B. Kim, Phys. Rev. **D60**, 095006 (1999), hep-ph/9906392.
[7] P. Langacker, Phys. Rev. **D58**, 093017 (1998), hep-ph/9805281.
[8] N. Arkani-Hamed, S. Dimopoulos, G. R. Dvali, and J. March-Russell, Phys. Rev. **D65**, 024032 (2002), hep-ph/9811448.
[9] K. Abazajian, G. M. Fuller, and M. Patel, Phys. Rev. Lett. **90**, 061301 (2003), hep-ph/0011048.
[10] T. Asaka, S. Blanchet, and M. Shaposhnikov (2005), hep-ph/0503065.
[11] K. Abazajian, G. M. Fuller, and M. Patel, Phys. Rev. **D64**, 023501 (2001), astro-ph/0101524.
[12] K. N. Abazajian and G. M. Fuller, Phys. Rev. **D66**, 023526 (2002), astro-ph/0204293.
[13] K. Abazajian, Phys. Rev. **D73**, 063506 (2006), astro-ph/0511630.
[14] P. Bode, J. P. Ostriker, and N. Turok, Astrophys. J. **556**, 93 (2001), astro-ph/0010389.
[15] T. Goerdt, B. Moore, J. I. Read, J. Stadel, and M. Zemp, Mon. Not. Roy. Astron. Soc. **368**, 1073 (2006), astro-ph/0601404.
[16] F. J. Sanchez-Salcedo, J. Reyes-Iturbide, and X. Hernandez (2006), astro-ph/0601490.
[17] M. I. Wilkinson et al. (2006), astro-ph/0602186.
[18] S. Tremaine and J. E. Gunn, Phys. Rev. Lett. **42**, 407 (1979).
[19] V. K. Narayanan, D. N. Spergel, R. Dave, and C.-P. Ma, Astrophys. J. **543**, L103 (2000), astro-ph/0005095.
[20] M. Viel, J. Lesgourgues, M. G. Haehnelt, S. Matarrese, and A. Riotto, Phys. Rev. **D71**, 063534 (2005), astro-ph/0501562.
[21] K. Abazajian, Phys. Rev. **D73**, 063513 (2006), astro-ph/0512631.
[22] U. Seljak, A. Makarov, P. McDonald, and H. Trac (2006), astro-ph/0602430.
[23] P. B. Pal and L. Wolfenstein, Phys. Rev. **D25**, 766 (1982).
[24] M. Drees and D. Wright (2000), hep-ph/0006274.
[25] A. D. Dolgov and S. H. Hansen, Astropart. Phys. **16**, 339 (2002), hep-ph/0009083.
[26] K. Abazajian, G. M. Fuller, and W. H. Tucker, Astrophys. J. **562**, 593 (2001), astro-ph/0106002.
[27] A. Boyarsky, A. Neronov, O. Ruchayskiy, and M. Shaposhnikov (2005), astro-ph/0512509.
[28] A. Boyarsky, A. Neronov, A. Neronov, O. Ruchayskiy, and M. Shaposhnikov (2006), astro-ph/0603368.
[29] A. Boyarsky, A. Neronov, O. Ruchayskiy, M. Shaposhnikov, and I. Tkachev (2006), astro-ph/0603660.
[30] S. Riemer-Sorensen, S. H. Hansen, and K. Pedersen (2006), astro-ph/0603661.
[31] C. Athanassopoulos et al. (LSND), Phys. Rev. Lett. **81**, 1774 (1998), nucl-ex/9709006.
[32] M. Sorel, J. M. Conrad, and M. Shaevitz, Phys. Rev. **D70**, 073004 (2004), hep-ph/0305255.
[33] P. Di Bari, Phys. Rev. **D65**, 043509 (2002), hep-ph/0108182.
[34] K. N. Abazajian, Astropart. Phys. **19**, 303 (2003), astro-ph/0205238.
[35] S. Dodelson, A. Melchiorri, and A. Slosar (2005), astro-ph/0511500.
[36] U. Seljak, A. Slosar, and P. McDonald (2006), astro-ph/0604335.
[37] K. Abazajian, N. F. Bell, G. M. Fuller, and Y. Y. Y. Wong, Phys. Rev. **D72**, 063004 (2005), astro-ph/0410175.
[38] A. Kusenko and G. Segre, Phys. Rev. **D59**, 061302 (1999), astro-ph/9811144.
[39] G. M. Fuller, A. Kusenko, I. Mocioiu, and S. Pascoli, Phys. Rev. **D68**, 103002 (2003), astro-ph/0307267.
[40] A. Kusenko, Int. J. Mod. Phys. **D13**, 2065 (2004), astro-ph/0409521.
[41] P. L. Biermann and A. Kusenko, Phys. Rev. Lett. **96**, 091301 (2006), astro-ph/0601004.
[42] M. Mapelli, A. Ferrara, and E. Pierpaoli (2006), astro-ph/0603237.
[43] B. W. O'Shea and M. L. Norman (2006), astro-ph/0602319.
[44] T. Asaka, A. Kusenko, and M. Shaposhnikov (2006), hep-ph/0602150.
[45] L. E. Strigari et al. (2006), astro-ph/0603775.
[46] A. D. Dolgov et al., Nucl. Phys. **B632**, 363 (2002), hep-ph/0201287.
[47] K. N. Abazajian, J. F. Beacom, and N. F. Bell, Phys. Rev. **D66**, 013008 (2002), astro-ph/0203442.
[48] Y. Y. Y. Wong, Phys. Rev. **D66**, 025015 (2002), hep-ph/0203180.
[49] D. A. Liedahl, A. L. Osterheld, and W. H. Goldstein, Astrophys. J. Lett. **438**, L115 (1995).
[50] W. W. Booyakasha (2006), private communication.
[51] S. Mashchenko, A. Sills, and H. M. P. Couchman (2005), astro-ph/0511567.
[52] J. F. Navarro, C. S. Frenk, and S. D. M. White, Astrophys. J. **462**, 563 (1996), astro-ph/9508025.
[53] A. Burkert, in *IAU Symp. 171: New Light on Galaxy Evolution*, edited by R. Bender and R. L. Davies (1996), pp. 175–+, astro-ph/9504041.
[54] A. Z. Bonanos, K. Z. Stanek, A. H. Szentgyorgyi, D. D. Sasselov, and G. A. Bakos, Astron. J. **127**, 861 (2004), astro-ph/0310477.
[55] R. P. van der Marel, D. R. Alves, E. Hardy, and N. B. Suntzeff, Astronom. J. **124**, 2639 (2002), astro-ph/0205161.
[56] D. R. Alves and C. A. Nelson, Astrophys. J. **542**, 789 (2000), astro-ph/0006018.
[57] A. Klypin, H. Zhao, and R. S. Somerville, Astrophys. J. **573**, 597 (2002), astro-ph/0110390.
[58] G. Battaglia et al., Mon. Not. Roy. Astron. Soc. **364**, 433 (2005), astro-ph/0506102.
[59] P. McDonald et al., Astrophys. J. Suppl. **163**, 80 (2006), astro-ph/0405013.
[60] S. Colombi, S. Dodelson, and L. M. Widrow, Astrophys.

J. **458**, 1 (1996), astro-ph/9505029.
[61] S. H. Hansen, J. Lesgourgues, S. Pastor, and J. Silk, Mon. Not. Roy. Astron. Soc. **333**, 544 (2002), astro-ph/0106108.
[62] M. Viel, J. Lesgourgues, M. G. Haehnelt, S. Matarrese, and A. Riotto (2006), astro-ph/0605706.
[63] M. Viel and M. G. Haehnelt, Mon. Not. Roy. Astron. Soc. **365**, 231 (2006), astro-ph/0508177.
[64] Abazajian, Fuller & Tucker [26] found a different limit due to a lower value of the central X-ray luminosity from the gas in Virgo. This had the effect of increasing the estimated signal to noise ratio. The resulting mass limit was therefore more stringent: $m_s < 8.2$ keV, using the production relation Eq. (2).